

# Influence of Residual Gas Composition and Background Pressure in a Multi-Stage Co-evaporation Chamber on the Quality of Cu(In,Ga)Se<sub>2</sub> Thin Films and Their Device Performance

Dieter Greiner, Jakob Lauche, Marc Daniel Heinemann, Volker Hinrichs, Helena Stange, Hengameh Allaf Navirian, Christian Kalus, Rutger Schlatmann, Christian A. Kaufmann

Helmholtz-Zentrum Berlin für Materialien und Energie, PVcomB, Schwarzschildstr. 3, 12489 Berlin, Germany

**Abstract** — Thin film solar cells with Cu(In,Ga)Se<sub>2</sub> (CIGSe) absorbers prepared by co-evaporation reach efficiencies above 21% [1]. Typical multi-stage co-evaporation chambers are MBE-like (ultra-)high vacuum systems with individual effusion sources for each element. Cleanliness of the process chamber and the background pressure during the co-evaporation process could be of importance for the chamber design and a fair comparison of production costs when comparing different PV/Chalcopyrite technologies.

Here we study the influence of the background pressure quality on the electronic and structural properties of the deposited absorber layer. To achieve this, we analyzed the residual gas composition before and the background pressure during consecutive co-evaporation processes and investigate the effect of a combined cleaning (mechanical and electro-chemical) of the chamber walls together with a simple conditioning of the chamber after opening the chamber and re-filling the crucibles.

Cleaning of the chamber yielded a significant reduction in carbon species and an overall lower base pressure. The background pressure during the process was reduced from  $\sim 6 \cdot 10^{-6}$  mbar (before cleaning with water cooling shroud) to  $1 \cdot 10^{-7}$  mbar (after cleaning with LN<sub>2</sub> filled cooling shroud). The type and amounts of contaminants in the absorber layer are characterized by laser ablation inductively coupled plasma mass spectroscopy (LA ICP-MS). The impact of the process pressure on the growth of the CIGSe layer is analyzed with respect to preferential orientation (using XRD), grain-size (using SEM), in-depth elemental gradients (using GDOES) and the electronic quality (using TRPL, *C-V*). Analysis of completed solar cell devices shows that the absorber band-gap is hardly affected by the chamber conditions, whereas we see an improved collection of charge carriers generated by photons in the infra-red spectral range from the conditioned chamber, also resulting in slightly higher  $j_{sc}$ . The major effect is an increase in median  $V_{oc}$  values from 585mV (before cleaning and conditioning) to 635mV (after cleaning and condition). The overall solar cell efficiency is increased by 18% (relative).

**Index Terms** — CIGSe co-evaporation, residual gas, contaminants.

## I. INTRODUCTION AND BACKGROUND OF THIS WORK

Thin film solar cells with Cu(In,Ga)Se<sub>2</sub> (CIGSe) absorbers prepared by co-evaporation reach efficiencies  $>21\%$  [1]. Typical multi-stage co-evaporation chambers are MBE-like (ultra-)high vacuum systems with individual effusion sources

for the elements. Cleanliness of the process chamber and the level of the background pressure during the co-evaporation process could be of importance for the chamber design and a fair comparison of production costs when comparing different PV/Chalcopyrite technologies.

## II. EXPERIMENTAL WORK

CIGSe thin films are grown via multi-stage co-evaporation in a physical vapor deposition (PVD) chamber. To transfer and accommodate the PVD chamber in a new laboratory, we performed several cleaning procedures:

1. Mechanical cleaning by pressure glass bead blasting to remove a millimeter thick Chalcogenide layer deposited on the chamber walls after several hundred deposition runs.
2. Chemically electro-polishing to remove oil contaminants and to reduce surface roughness after the bead blasting.

During normal operation the chamber gets “conditioned” after every maintenance, where the crucibles are re-filled, windows are cleaned and loose deposited material at walls is removed. Conditioning means that the chamber walls are baked-out, the substrate heater temperature is set to above the growth temperature and the sources are heated slightly above their evaporation temperatures. This procedure leads to less variations in the processes conditions due to lower background pressure, owing mainly to the reduction of water and carbon species at different pressure conditions.

Four multi-stage evaporation processes with nominally identical growth recipe (layer thickness, elemental fluxes) were performed under different PVD chamber conditions: (1) before chamber cleaning and before conditioning of the chamber; (2) before cleaning, but after conditioning, (3) after cleaning, without conditioning and (4) after cleaning, after conditioning. After substrate loading and heating the substrates to 250°C (the starting temperature for the process) and after the effusion cells are approx. 50K below evaporation temperature, we recorded the partial pressure in the range of 1-200 atomic mass units (amu) with a Stanford Research residual gas analyzer (RGA200). The RGA200 is attached to

TABLE I  
SAMPLE PREPARATION AND CIGSE ABSORBER PROPERTIES, THAT WERE GROWN IN THE PRESENTED PROCESSES.

Process	Absorber properties									
	Average process pressure (mbar)	Virtual contamination layer	$I_{(220/204)} / I_{(112)}$ compared to powder	PL life-time	Atomic concentration (ppm) with > 1ppm					
					B	Ti	Zn	Pd	Ag	Cd
1 (before cleaning, before conditioning)	$6.9 \cdot 10^{-6}$	4.8 $\mu\text{m}$	1.4	-	6.5	0.9	2.8	6.7	0.1	8.0
2 (before cleaning, after conditioning)	$6.1 \cdot 10^{-7}$	0.4 $\mu\text{m}$	1.5	-	2.9	5.1	5.0	8.2	0.0	10.2
3 (after cleaning, before conditioning)	$1.1 \cdot 10^{-5}$	7.1 $\mu\text{m}$	0.3	43 ns	4.3	0.9	2.6	8.7	0.7	11.0
4 (after cleaning, after conditioning)	$4.9 \cdot 10^{-7}$	0.3 $\mu\text{m}$	1.4	13 ns	4.3	0.1	5.7	8.3	2.8	10.8

the chamber, but can be shuttled off by a valve for protection during deposition.

CIGSe thin films are deposited onto Mo coated glass substrates (Diamant, St. Gobain) with a  $\text{SiO}_x\text{N}_y$  alkaline diffusion barrier at a maximum nominal process temperature of 530°C. To avoid sodium related growth effects during the formation of the CIGSe and in order to see the bare effect of the chamber conditions, sodium was only supplied by a NaF post deposition treatment, where 25nm NaF were deposited in a Se atmosphere for 20min during cooling down of the substrate temperature from 530°C to 300°C. Laser light scattering, infra-red light reflectometry (ILR) and pyrometry were used for process control.

Complete solar cell devices (glass/ $\text{SiO}_x\text{N}_y$ /Mo/CIGSe/CBD-CdS/i-ZnO/ZnO:Al/Ni-Al-Ni grid) were fabricated and characterized by I-V and external and internal quantum efficiency measurements to assess the quality of the deposited material. Dismantling, cleaning, moving and mounting the system in the new laboratory took several months. Therefore the time period between the two processes before and after cleaning was approx. one year. To achieve a good comparison between the two processes before and after cleaning, we used the same Mo-glass substrates and nominally identical CdS deposition and TCO sputter processes. We assume little degradation or shifts in these processes. It was not possible to use the same grid metallization chamber and scribing facility. Thus, comparability is better for the processes with and without conditioning than before and after cleaning. For a fair comparison of the effect of the cleaning procedure, the mentioned changes of the manufacturing process must be taken into account.

The type and amounts of contaminants in the absorber layer are characterized by LA ICP-MS. The impact of the process pressure on the growth of the CIGSe layer is analyzed with respect to preferential orientation (XRD), grain-size (SEM), in-depth elemental gradients (GDOES) and the electronic quality by time-resolved PL and admittance spectroscopy. The elemental depth profiles of the CIGSe layer were measured by

glow discharge optical emission spectroscopy (GDOES) with a GDA650 apparatus from Spectrumba using a pulsed RF Ar plasma for sputtering. The quantitative analysis was done with a matrix calibration scheme using an independently measured one-stage grown CIGSe sample with flat atomic profiles and similar concentration as the investigated CIGSe layers.

### III. EXPERIMENTAL RESULTS

#### A. Effect of Cleaning and Conditioning on Residual Gas and Total Process Pressure

Fig. 1 shows the partial pressures right before the process starts. The cleaning of the chamber yielded a cleaner vacuum with no pressure peaks with masses above 100amu. The characteristic mass peak at 69 amu originates from Fomblin oil in an earlier used pre-pump; it is reduced by two orders of magnitude after cleaning compared to the uncleaned chamber -

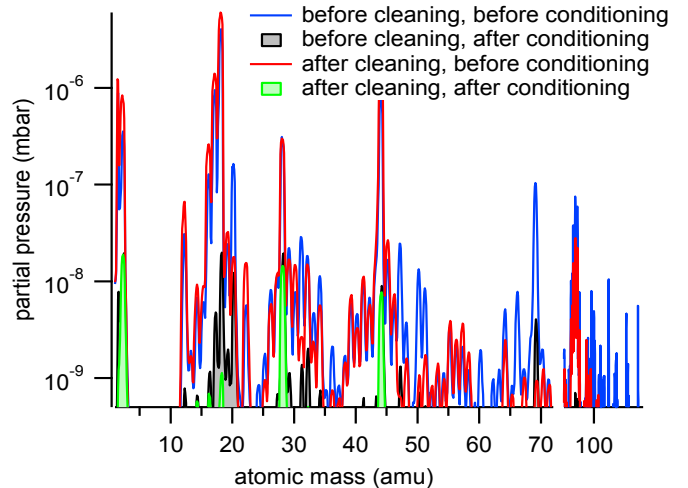


Fig. 1. Partial pressures in dependence of the atomic mass right before process starts; i.e. after substrate loading and substrate heating to 250°C; effusion cells approx. 50K below evaporation temperature. Note, linear abscissa scale for masses to 72 amu and logarithmic scale for masses up to 180amu.

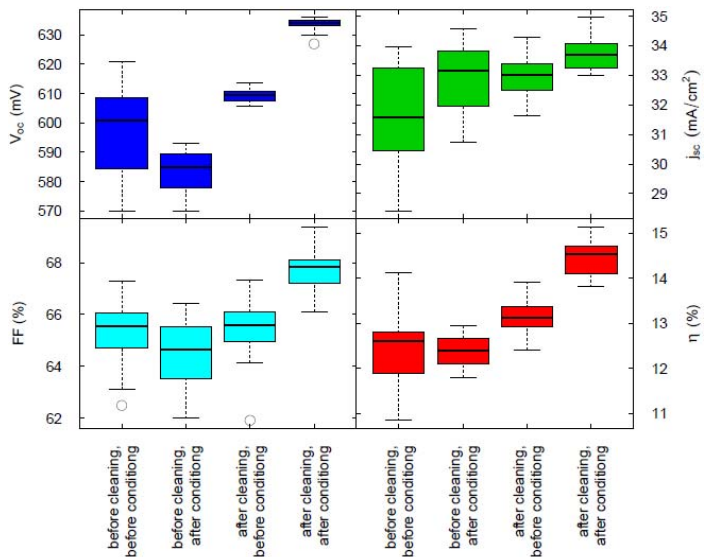


Fig. 2. Boxplot representation of the main IV parameters short circuit current density ( $j_{sc}$ ), open circuit voltage ( $V_{oc}$ ) fill factor (FF) and efficiency ( $\eta$ ) for up to 15 solar cells on a substrate from each co-evaporation process.

even before conditioning. It is worth to mention that a higher hydrogen partial pressure was detected in the chamber after cleaning, which we attribute to the higher desorption rate of hydrogen from the steel chamber walls. That is often seen in ‘fresh’ steel surfaces, especially when they are not baked out, which was not possible in our case. After several depositions, we see a steady decrease of hydrogen inside the chamber. To additionally reduce the hydrogen pressure within the chamber, a set-up of two dry pre-pumps - one with a higher base pressure but lower partial pressure for hydrogen - was used.

Conditioning the chamber after maintenance yields a significant reduction of water (18, 17 amu), C/CO/CO<sub>2</sub> species (12, 28, 44 amu) and all higher masses (>44amu), both before and after chamber cleaning.

To protect the residual gas analyzer from deposition, the partial pressures were not monitored during the deposition process. However the total pressures during the co-evaporation process was recorded and the average total pressure during the deposition process is listed in Table I. Considering Langmuir’s law, i. e. the deposition rate of a gas with a pressure of  $10^{-6}$  mbar and a sticking coefficient of 1 is approximately  $1 \text{ \AA/s}$ , we can estimate the maximum contaminated layer thickness during the deposition process, assuming that all gas species condensate in the growing absorber film during the process period (see also Table I). Conditioning of the chamber after maintenance has a strong effect on the background pressure and thus the potential contribution of contaminants to the absorber thickness during growth. This estimate is obviously too high, but gives a good indication of the dynamics within

the chamber. In the process after cleaning, but without conditioning, the process pressure was two orders of magnitude higher than after bake-out, also because the cooling shroud was intentionally not filled with LN<sub>2</sub> in order to enhance the outgassing effect.

### B. Effect on Solar Cell Performance

As seen in the IV measurements (Fig. 4), all relevant IV parameters ( $j_{sc}$ ,  $V_{oc}$ , FF) increase after proper cleaning and preconditioning, resulting in overall average solar cell efficiency increase by 18% (relative). The major effect is an increased median  $V_{oc}$  value of 635mV (after cleaning and conditioning) from initially 585mV (before cleaning and conditioning).

External quantum efficiency (EQE) analysis of completed solar cell devices (Fig. 3) show that the band-gap is hardly affected by the chamber’s condition. However, we see a higher EQE in the infra-red spectral range from the conditioned chamber, also resulting in slightly higher  $j_{sc}$ . To investigate this effect in detail, we measured the reflectance R of the solar cell and calculated the internal quantum efficiency IQE = EQE/(1-R), which is also plotted for the samples after cleaning in Fig. 3. From the IQE, we can conclude that the higher IQE in the long wavelength regime is not a window layer effect, but is really the result of an improved collection of charge carriers after conditioning. This finding points to a longer minority charge carrier lifetime / diffusion length for the CIGS layer deposited in the cleaned and conditioned chamber. However, the results of the time-resolved PL life-time measurement at room temperature (see Table I) show a shorter lifetime for the sample from the process after conditioning. As discussed by Maiberg et. al [2] the TRPL measurement at room temperature probes the combined life-time of different radiative decay.

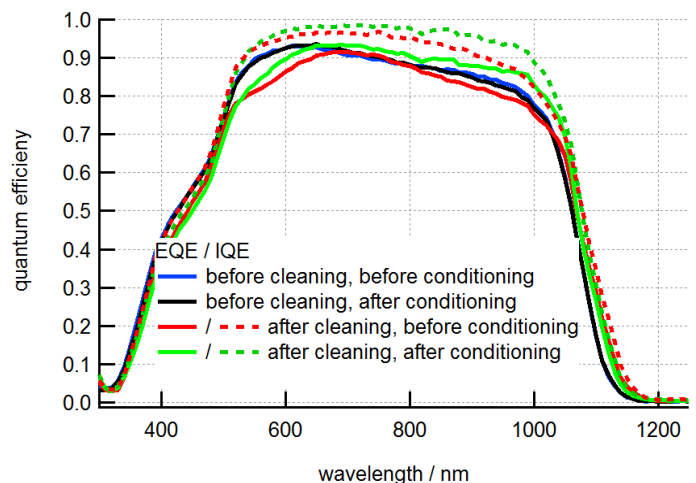


Fig. 3. External (EQE) and internal (IQE) quantum efficiency of the best solar cell from each deposition run.

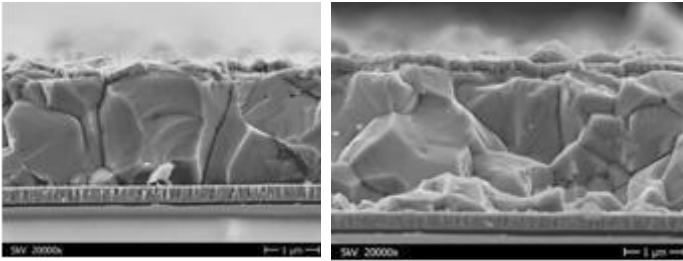


Fig. 4. Scanning electron micrograph cross section of the solar cell device (left) before and (right) after chamber cleaning both before conditioning.

Hence, the shorter lifetime after conditioning could point to a reduced defect states in the band-gap of the absorber.

### C. Effect on Absorber Properties

In the following, we discuss the effect of the different preparation conditions on the absorber quality.

The effect of cleaning and conditioning on the presence of trace elements within the grown CIGSe layer was measured by LA ICP-MS. Elements – apart from Cu, In, Ga, Se, Na - with concentrations above 1ppm are boron, titanium, zinc, palladium, silver and cadmium (see Table I). To discuss the contaminations, one has to keep in mind that a 5N evaporation material has a range of different contaminants with a concentration of 1ppm. We use a 6N pure source material for Cu, In, Se and for Ga a 7N pure material. Assuming a homogeneous distribution of the impurities during the evaporation process and full implementation of the impurities into the growing film, the impurities from the evaporates have a concentration  $< 0.1$ ppm. Hence, the detected impurities listed in Table I should be deduced to originate from the PVD chamber (or sample handling before and after the deposition process). Boron is used in the PBN crucibles and the PBN diffusor plate in front of the substrate heater. The higher B concentration after chamber cleaning may be a result of renewed crucibles and a B-concentration reduction might be visible only after a couple of conditioning sequences. The origin of Ti and Pd is not clear. We assume that Cd and Zn originate from the sample handling; however we not bother as they are present in the Chalcopyrite solar cell anyway.

Figure 4 compares SEM images of the two absorber layers before and after cleaning under the unfavorable growth conditions prior to conditioning. No significant difference in the grain size and grain distribution can be seen. (In the SEM micrograph after cleaning, white ‘crumbs’ can be seen. However, it is not clear, what they are.)

A main effect of the conditioning after cleaning is a higher CIGSe (220,204)/112 XRD integral peak ratio (see. Fig. 5). According to the model of Chaisitsak et al [3] a 220/204

orientation is favorable, because Cd atoms can better bond/penetrate into the CIGSe surface during CdS chemical bath deposition of the buffer layer and a higher FF can be achieved. Compared to a randomly oriented CIGSe powder (JCPDS card 01-081-1936) we measure slightly  $\{220\}/\{204\}$  preferentially orientated grains for three of the four samples. Only the sample from the process after cleaning but without conditioning shows a marked 112 preferential orientation (see Table I). The observed fill factor effect is in accordance to the model of Chaisitsak. By favoring a 220/204 orientation a higher background-pressure seems to have a similar effect as a low selenium to In/Ga flux ratio in the first stage of the process [3]-[4].

In-depth elemental gradients of the absorber layer were measured by GDOES. With the expression to calculate the band-gap energy in dependence of  $x$ : =GGI [5]

$$E_g(x) = (1-x) 1.01\text{eV} + x \cdot 1.65\text{eV} - 0.15x(1-x), \quad (1)$$

we calculate the profiles of the band-gap energy (Fig. 6). After conditioning the CIGSe layer show less pronounced band-gap gradients towards the back and front contact indicating a higher In-Ga interdiffusion during the growth process compared to the growth under higher vacuum pressure before conditioning. The origin of the steeper front contact band-gap gradients after cleaning is not clear, it might be caused by a shift of the evaporation rate ratio of the In and Ga source.

The Na concentration, shown in the lower part of Fig 6, increases due to chamber cleaning and decreases after conditioning. Thus, we speculate that due to less carbon contaminants after cleaning, the Chalcopyrite lattice has the capability to incorporate more Na atoms. This effect is enhanced by a non-conditioned chamber, when more O and water is present during the growth process.

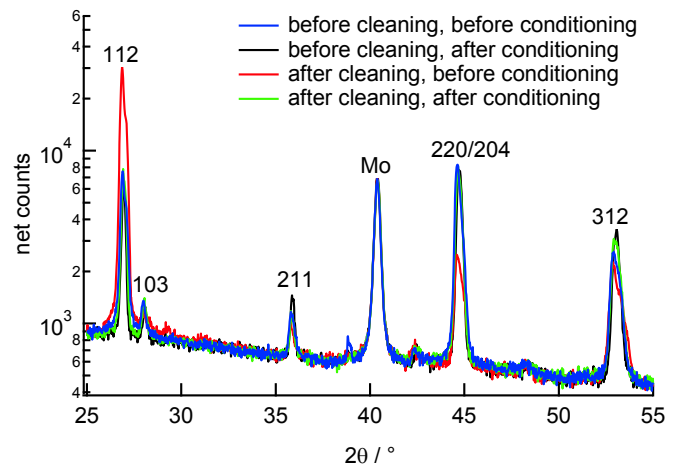


Fig. 5. X-ray diffraction pattern in Bragg-Brentano geometry with the main CIGSe peaks of the absorber layer from each process.



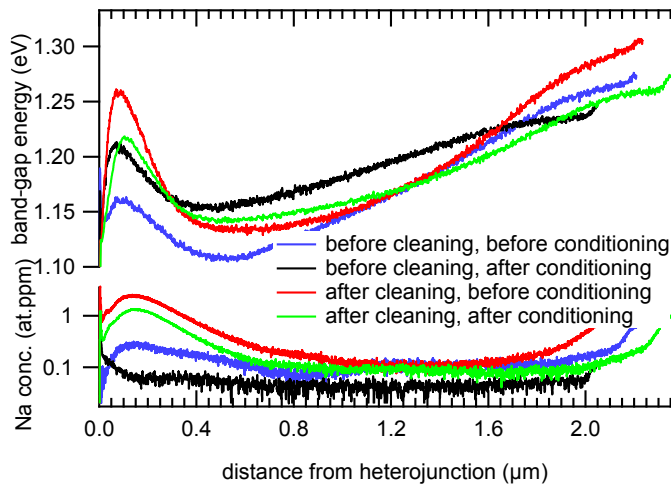


Fig. 6. GDOES depth profiles of the band-gap energy (above) and Na concentration (below) of the CIGSe layer from each deposition run.

To clarify this question, we measured the capacitance at 10kHz. The carrier concentrations obtained from the voltage dependency of the capacitance ( $C-V$ ) [6] are plotted in Fig. 7. The absorber prepared after cleaning and after conditioning, which has the highest  $V_{oc}$  and cell performance, shows the lowest carrier concentration of  $2 \cdot 10^{15} \text{ cm}^{-3}$ . This proves that the high  $V_{oc}$  does not originate from the high doping level. The highest  $C-V$  carrier concentration is measured for the cell prepared in the cleaned chamber, prior to conditioning, which also had the highest exposure to contaminants during the deposition process (see highest thickness of virtual contamination layer in Table I) and which has also the highest Na concentration. Thus, we conclude that the higher capacitance originates from a high defect density, caused by the presence of contaminants and possibly other Chalcopyrite-compound based defects. The effect of Na may be strongly dependent on the presence of different contaminants and may be a subject of further study.

#### IV. SUMMARY

In this work, we studied the influence of the background pressure level and residual gas composition on the electronic and structural properties of the deposited CIGSe absorber layer and its impact on the device performance. We show that all relevant IV parameters ( $j_{sc}$ ,  $V_{oc}$ , FF) increase by proper cleaning and preconditioning, resulting in overall average solar cell efficiency increase by 18% (relative). The cleaning of the evaporation chamber yields a significant reduction of carbon species and the preconditioning a much lower deposition pressure. Thereby the growth of the CIGSe layer is

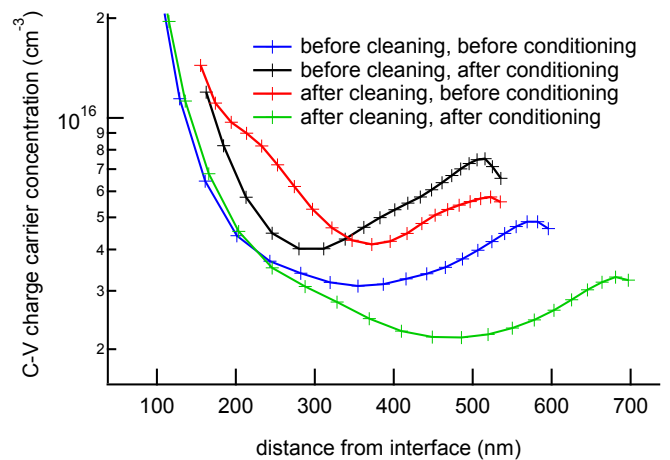


Fig. 7. Charge carrier concentration obtained from capacitance-voltage ( $C-V$ ) measurements in dependence of the distance from the hetero-interface measured at 10kHz. For comparison, solar cells with the same area and with a parallel resistance  $> 1\text{k}\Omega$  of each process were chosen.

affected both structurally and electronically: we found a slightly 220/204 preferentially orientated CIGSe grains. Also, the In/Ga interdiffusion is enhanced. More sodium can be implemented in the CIGSe layer after the chamber cleaning. An improved collection of charge carriers is obtained from QE measurements, which indicates a longer minority charge carrier lifetime/diffusion length for the CIGS layer deposited in the cleaned and conditioned chamber.

#### ACKNOWLEDGEMENT

Technical assistance by S. Cinque, T. Kodalle for GDOES measurements; C. Klimm for SEM, D. Erfurt for optical measurements; B. Bunn, I. Dorband, C. Ferber, T. Münchenberg and M. Kirsch for substrate preparation, front contact, buffer and window layer deposition is greatly acknowledged. The authors thank everybody who was involved in moving the PVD system and building-up the new laboratory, especially we would like to mention K. Priezel, T. Münchenberg and P. Loche.

#### REFERENCES

- [1] P. Jackson, D. Hariskos, R. Würz et al., *Phys. Status Solidi*, 1-4 (2014).
- [2] M. Maiberg, T. Hölscher, S. Zahedi-Azad, R. Scheer, "Theoretical study of time-resolved luminescence in semiconductors. III. Trap states in the band gap", *J. Appl. Phys.*, 118, 105701, 2015
- [3] S. Chaisitsak, A. Yamada, M. Konagai, *Jpn. J. Appl. Phys.*, 41, 507, 2002
- [4] D. Greiner, J. Lauche, S. Harndt et al, *Proceedings of the 42nd IEEE PVSC*, 2015

[5] S. Ishizuka, K. Sakurai, A. Yamada, H. Shibata, K. Matsubara, M. Yonemura, S. Nakamura, H. Nakanishi, T. Kojima, S. Niki, "Progress in the Efficiency of Wide-Gap Cu(In<sub>1-x</sub>Ga<sub>x</sub>)Se<sub>2</sub> Solar Cells Using CIGSe Layers Grown in Water Vapor", *Jpn. J. Appl. Phys.*, 44, L679, 2005

[6] J. Hilibrand, RD. Gold, "Determination of the impurity distribution in junction diodes from capacitance-voltage measurements", *RCA review* 21,2, 245, 1960